Biochimica et Biophysica Acta 1840 (2014) 2989–2999

Contents lists available at ScienceDirect

Biochimica et Biophysica Acta

journal homepage: www.elsevier.com/locate/bbagen

Picosecond dynamics in haemoglobin from different species: A quasielastic neutron scattering study

Andreas M. Stadler [a,*], Christopher J. Garvey [b], Jan Peter Embs [c], Michael Marek Koza [d], Tobias Unruh [e,f], Gerhard Artmann [g], Giuseppe Zaccai [h]

[a] Jülich Centre for Neutron Science (JCNS) and Institute of Complex Systems (ICS), Forschungszentrum Jülich GmbH, 52425 Jülich, Germany
[b] Australian Nuclear Science and Technology Organisation, Locked Bag 2001, Kirrawee DC, New South Wales 2232, Australia
[c] Laboratory for Neutron Scattering and Imaging, Paul Scherrer Institut, 5232 Villigen PSI, Switzerland
[d] Institut Laue-Langevin, CS 20156, 38042 Grenoble, France
[e] Technische Universität München, Physik Department E13 and Forschungs-Neutronenquelle Heinz Maier-Leibnitz (FRM II), Garching bei München, Germany
[f] Friedrich-Alexander-Universität Erlangen-Nürnberg, Physik Department, Lehrstuhl für Kristallographie und Strukturphysik, Erlangen, Germany
[g] FH Aachen, Institute for Bioengineering, Heinrich-Mußmann-Straße 1, 52428 Jülich, Germany
[h] Institut Laue-Langevin and CNRS, CS 20156, 38042 Grenoble, France

ARTICLE INFO

Article history:
Received 10 March 2014
Received in revised form 10 June 2014
Accepted 11 June 2014
Available online 19 June 2014

Keywords:
Haemoglobin
Body temperature adaptation
Protein dynamics
Picosecond dynamics
Quasielastic neutron scattering

ABSTRACT

Background: Dynamics in haemoglobin from platypus (*Ornithorhynchus anatinus*), chicken (*Gallus gallus domesticus*) and saltwater crocodile (*Crocodylus porosus*) were measured to investigate response of conformational motions on the picosecond time scale to naturally occurring variations in the amino acid sequence of structurally identical proteins.
Methods: Protein dynamics was measured using incoherent quasielastic neutron scattering. The quasielastic broadening was interpreted first with a simple single Lorentzian approach and then by using the Kneller–Volino Brownian dynamics model.
Results: Mean square displacements of conformational motions, diffusion coefficients of internal dynamics and residence times for jump-diffusion between sites and corresponding effective force constants (resilience) and activation energies were determined from the data.
Conclusions: Modifications of the physicochemical properties caused by mutations of the amino acids were found to have a significant impact on protein dynamics. Activation energies of local side chain dynamics were found to be similar between the different proteins being close to the energy, which is required for the rupture of single hydrogen bond in a protein.
General significance: The measured dynamic quantities showed significant and systematic variations between the investigated species, suggesting that they are the signature of an evolutionary adaptation process stimulated by the different physiological environments of the respective protein.

1. Introduction

Haemoglobin (Hb) is the main macromolecular component of red blood cells. Its biological function is to transport oxygen from lung to tissue, where it is needed for metabolism. Hb from higher species is assembled into a tetramer with a molecular mass of approximately 64 kDa. The tetramer is composed of two so-called α-chains and two β-chains, which are not identical but structurally very similar. From this perspective Hb can be seen as a dimer of dimers. Each chain is predominantly composed of α-helices and holds one heme group in a cavity, to which oxygen and several other small molecules can bind reversibly. Binding and release of oxygen to Hb is highly cooperative [1]; it enables oxygen saturation in the lungs and an efficient deposition in the capillaries. Hb also served as a prototype for the investigation of an allosteric mechanism in proteins [2–4].

In more recent studies, circular dichroism and dynamic light scattering experiments revealed a direct correlation of a partial unfolding transition with body temperature of different species [5,6]. The transition is accompanied by an onset in protein association. Interestingly, the interpretation emerged that the effect is caused by specific physicochemical properties of the Hb macromolecules in a way that each protein acts as a molecular thermometer adapted to the respective body temperature of the species [7]. Temperature dependent micropipette aspiration experiments on single human red blood cells revealed a passage transition through a narrow capillary in a narrow temperature range close to human body temperature, following a phase transition in the highly

* Corresponding author. Tel.: +49 2461614502; fax: +49 2461612610.
E-mail address: a.stadler@fz-juelich.de (A.M. Stadler).

http://dx.doi.org/10.1016/j.bbagen.2014.06.007
0304-4165/

concentrated Hb solution in the cells from a gel-like to a fluid state [8]. It was suggested that the loss of secondary structure content and the onset of protein aggregation [9], effects occurring on a molecular level, could be at the origin of the phase transition and cause the macroscopic cellular effect [7]. In a previous study we have investigated the dynamics of human Hb in whole red blood cells [10,11] and the role of hydration on these motions [12] by neutron spectroscopy. Results revealed a correlation between protein resilience, melting temperatures and average body temperatures of Hb from different species on the nanosecond time scale [13].

The biological function of Hb is determined by its three-dimensional structure and dynamics, which play an equally important role. Molecular forces need to be sufficiently strong to keep the protein in the folded conformation and to prevent unfolding, while a certain flexibility of the structure is necessary for biological function [14]. In Hb and the structurally related myoglobin, for example, there does not exist a static channel through which the oxygen can move directly to its binding site at the heme group. Instead, the oxygen molecule diffuses through a pathway of transient channels, which open and close as a consequence of dynamic conformational rearrangements [15]. A static Hb structure without conformational flexibility would not be biologically active. Dynamics in biological macromolecules occur over a very broad range of time scales [16]: Fast motions of amino acid side chains and methyl groups happen on the picosecond time scale, while slower reorientations of whole side chains, fluctuations of the backbone and of secondary structure elements extend into the nanosecond time range. Diffusive motions of whole protein domains occur at times from some tens up to hundreds of nanoseconds, whereas folding and assembly of a protein into its correct three-dimensional structure occurs on the micro- to millisecond level. Neutron spectroscopy is a well-suited and established technique to probe the dynamics of biological macromolecules on the picosecond to nanosecond time scale [17,18]. Incoherent quasielastic neutron scattering (QENS) yields the relevant information about the spatial extent and the relaxation times of the molecular motions as a function of the scattering vector [19]. The incoherent scattering cross section of hydrogen is the largest of all elements that occur in biological matter including deuterium [20]. Therefore, hydrogen atoms are reporters for average protein dynamics as they are uniformly distributed in biomacromolecules. The characteristics of the neutron time-of-flight spectrometers in this study allowed the investigation of protein motions with relaxation times of up to several tens of picoseconds and amplitudes of some Ångstroms.

In this article we report on a comparative QENS study of picosecond dynamics of Hb from platypus (*Ornithorhynchus anatinus*), chicken (*Gallus gallus domesticus*) and crocodile (*Crocodylus porosus*) Hb measured by neutron time-of-flight spectroscopy. The scientific aim was to investigate if picosecond dynamics in the proteins are sensitive to the physicochemical differences caused by modifications in the amino acid sequences. The different dynamic parameters extracted showed clear differences between the investigated species that might reflect adaptation to the physiological environment of the proteins.

2. Material and methods

2.1. Sample preparation

Blood samples of platypus, chicken and saltwater crocodile were obtained from live animals. Red blood cells were harvested by centrifugation and washed several times with isotonic buffer. The platypus red blood cells were then lysed by adding distilled water and centrifuged at 20,000 relative centrifugal force (rcf) to remove membrane fragments. Crocodile and chicken red blood cells are nucleated and were lysed with a lysis buffer (0.5% Tris–HCl at pH 7.5) to avoid breaking the nuclear membrane. Nuclei were separated by centrifugation at 2800 rcf and the supernatant was consecutively spun at 20,000 rcf. The Hb solutions were dialysed against distilled water before lyophilization. The dried Hb powders were dissolved in 99.9% D_2O incubated for half a day to exchange the labile H atoms and before being freeze dried. For the neutron experiments, highly concentrated Hb solutions corresponding to protein concentrations of 570 mg/ml using the reported specific partial volume of Hb 0.75 cm^3/g [21] were prepared. The dry Hb powders were placed in flat 0.3 mm thick aluminium sample holders. D_2O buffer (0.1 M KCl, 61.3 mM K_2HPO_4, 5.33 mM KH_2PO_4, pD 7.4) was then added to a level of 1.1 g D_2O/1 g Hb. The comparatively large amount of D_2O was chosen as we showed before that one hydration layer, which is typically used in hydrated powder samples, is not sufficient to activate all conformational fluctuations in proteins [12,13]. The sample holders were then hermetically sealed and incubated in the fridge at ~6 °C to allow for equilibration of the humidity. The amounts of Hb in the sample cells were: 101 mg for platypus Hb, 202 mg for chicken Hb, and 152 mg for crocodile Hb. It was checked by weighing that no loss of sample material occurred during the neutron scattering experiments.

2.2. QENS experiments

The experiments were performed on the cold neutron time-of-flight spectrometers IN6 at the Institut Laue-Langevin (ILL, Grenoble, France) [22], TOFTOF at the Heinz Meier-Leibnitz Zentrum (MLZ, Garching, Germany) [23], and FOCUS at Paul Scherrer Institut (PSI, Villigen, Switzerland) [24]. On IN6 and TOFTOF the incident wavelengths were set to 5.1 Å. An incident wavelength of 5.0 Å was chosen on FOCUS. On TOFTOF the chopper speed and the chopper ratio were set to 12,000 rpm and 4, respectively. The settings resulted in similar energy resolutions of approximately 100 μeV (full-width at half-maximum) and an identical covered scattering vector range on all spectrometers. All samples, including the vanadium slab and empty sample holder, were oriented at 135° with respect to the incident neutron beam direction. The measured spectra were corrected for energy dependent detector efficiency, empty cell scattering, normalized to vanadium, and transformed into energy transfer and scattering vector space. The spectra of the individual detectors were binned into groups for better statistics. Multiple scattering was neglected as the transmissions of all samples were around 0.9. The incoherent scattering cross section ratio of Hb in the concentrated solutions was estimated to be >96% [12], so that we could neglect the contribution of D_2O solvent to the measured data.

2.3. QENS data analysis

A thorough description of the QENS technique can be found in the book of Bée [19]. In general, the theoretical incoherent quasielastic scattering function $S(q, \omega)$ due to diffusive molecular motions in soft condensed matter can be written as [19]

$$S(q,\omega) = A_0(q) \times \delta(\omega) + \sum_{n=1}^{N} A_n(q) \times L_n(q,\omega), \quad (1)$$

where $A_0(q)$ is the elastic incoherent structure factor (EISF), which contains detailed information about the geometry of molecular motions that are confined with respect to the length-time resolution of the spectrometer; the following summation describes the quasielastic broadening interpreted as N Lorentzians, the number N depending on the model chosen.

In the simplest model, the QENS spectra can be interpreted according to Eq. (2).

$$S(q,\omega) = A_0(q) \times \delta(\omega) + (1 - A_0(q)) \times L(q,\omega), \quad (2)$$

where the first term is the elastic scattering dominated by hydrogen atoms that are localized within the length-time scale of the

experiment and one effective Lorentzian is fitted to the quasielastic broadening [17]. The Lorentzian has the form

$$L(q,\omega) = \frac{1}{\pi}\cdot\frac{\Gamma(q)}{(\hbar\omega)^2+\Gamma(q)^2}, \tag{3}$$

where $\Gamma(q)$ is the half-width at half-maximum. The scattering function $S(q,\omega)$ plus linear background $B(\omega)$ was convoluted with the instrumental resolution function $S_{res}(q,\omega)$ and fitted to each measured spectra $S(q,\omega)_{meas}$ (individual fitting procedure) according to

$$S_{meas}(q,\omega) = \left[\exp\left(-\left\langle x^2{}_{vib}\right\rangle q^2\right)\times S(q,\omega)+B(\omega)\right]\otimes S_{res}(q,\omega). \tag{4}$$

Mean square displacements of fast vibrational motions $\langle x_{vib}{}^2\rangle$ were taken into account by a Debye–Waller factor. The fits were performed over the energy transfer range from −1.5 meV to +1.5 meV. Each instrumental resolution function $S_{res}(q,\omega)$ was determined by measuring a vanadium standard sample.

In an alternative approach, the data were fitted by a model due to Kneller–Volino [25,26] applying a Gaussian localization function for the diffusing particles. The theoretical scattering function for Brownian dynamics in a quasi-harmonic potential is given by

$$S(q,\omega) = A_0(q)\delta(\omega)+\sum_{n=1}^{\infty}A_n(q)\times\frac{1}{\pi}\frac{\left(n\hbar D_{eff}/\left\langle x^2\right\rangle\right)}{\left(n\hbar D_{eff}/\left\langle x^2\right\rangle\right)^2+(\hbar\omega)^2}, \tag{5}$$

with

$$A_0(q) = e^{-\langle x^2\rangle q^2}(1-p)+p \tag{6}$$

as the EISF and the prefactors

$$A_n(q) = e^{-\langle x^2\rangle q^2}(1-p)\frac{\left(q^2\left\langle x^2\right\rangle\right)^n}{n!} \tag{7}$$

of the Lorentzians describing the quasielastic broadening [25,26]. D_{eff} is an effective diffusion coefficient for the observed molecular motions. The fraction p needs to be included to account for hydrogen atoms that move too slowly to be resolved in the time scale of the spectrometer and will therefore appear to be immobile. Their scattering function is constant with q. In the case that the granularity of molecular motions becomes visible by the spatial resolution of the neutron spectrometer the diffusive motions are better described by a scenario of small jumps between different sites with a residence time τ between each jump. In that case the q-dependence of the effective diffusion coefficient can be described effectively by the jump-diffusion mechanism with

$$D_{eff}(q) = \frac{D}{1+Dq^2\tau} \tag{8}$$

and the jump-diffusion coefficient D and the residence time τ [19,26]. During data analysis the model for Brownian dynamics in a quasi-harmonic potential was convoluted with the resolution function and fitted simultaneously to the whole data set (global fitting procedure) including a Debye–Waller factor for vibrational motions and a linear background for each spectrum as in Eq. (4). The summation was performed up to $N = 50$, above that limit no changes in the fits were observed. In the case that the diffusive motions would be described by a q-independent diffusion coefficient, the fits would have converged with $\tau \to 0$.

Effective force constants $<k'>$ were determined from the slope of $<x^2>$ versus temperature according to

$$\langle k'\rangle = \frac{0.00046}{\Delta\langle x^2\rangle/\Delta T} \tag{9}$$

[14,27], and from the Kneller–Volino model with respect to the shape of the confining Gaussian function [25]. The units of $<k'>$ are in N/m when $<x^2>$ is in Å^2 and T is in K.

2.4. Multiple sequence alignments

Protein amino acid sequences were obtained from the NCBI gene and protein databases (human Hb HBA_HUMAN P69905 and HBB_HUMAN P68871; platypus Hb HBA_ORNAN P01979 and HBB_ORNAN P02111; chicken Hb HBA_CHICK P01994 and HBB_CHICK P02112; crocodile Hb HBA_CRONI P01998 and HBB_CRONI P02129). Multiple sequence alignments were performed using the CLUSTAL W software [28]. The α-helical content of the subunits was calculated using the Jpred3 secondary structure prediction server [29].

3. Results

The dynamics of the different samples in the picosecond time-scale was studied using various neutron time-of-flight spectrometers: platypus Hb was measured on TOFTOF at MLZ, chicken Hb on the instrument IN6 at ILL, and crocodile Hb on the FOCUS spectrometer at PSI. All neutron spectrometers were operated using similar energy resolutions, thus, being sensitive to the same dynamic processes. Representative QENS spectra of the different samples at the scattering vector $q = 1.8$ Å^{-1} are shown in Fig. 1.

First, we describe the analysis of the QENS data using Eq. (2). The measured spectra could be well described with a δ-function and one phenomenological Lorentzian for the quasielastic broadening plus flat background. The flat background accounts for low frequency vibrational motions. The contribution and q-dependence of the background is very similar between the three different samples at the same temperatures. As an example, we show the q-dependent relative contribution of the background at different temperatures for platypus Hb in Fig. 2. The background increased as a function of q^2, as it is expected for vibrational motions.

The phenomenological EISFs, which contain information about the amplitudes of motions of the different samples, are shown in Fig. 3 at selected temperatures. The EISF could be interpreted well using the Gaussian approximation according to

$$A_0(q) = e^{-\langle x^2\rangle q^2}(1-p)+p, \tag{10}$$

where $<x^2>$ is the mean square displacement (MSD) of the observed motions and p is the fraction of protons, which are too slow and appear as immobile within the time resolution of the neutron spectrometer. The theoretical function deviates slightly from the EISF at the highest temperatures. It was pointed out that the shape of the EISF of proteins can be better described by a $<x^2>$ distribution instead of a single average MSD value [12,30–33]. This is certainly the case considering the heterogeneity of protein dynamics. However, for the analysis of Hb dynamics in the picosecond time scale described in this work using a $<x^2>$ distribution instead of a single average $<x^2>$ does not improve the quality of the fits. Therefore, for simplicity we chose the standard Gaussian approximation for the interpretation of the EISFs.

The obtained MSD and the fractions of immobile hydrogens of all investigated samples are shown in Fig. 4. Effective force constants $<k'>$ were determined from the temperature evolution of the MSD in temperature ranges below and above the body temperatures of platypus Hb and chicken Hb (vertical dashed lines in Fig. 4). The results are summarized in Table 1.

The half-widths $\Gamma(q)$ of the quasielastic broadening of the samples are presented in Fig. 5 as a function of the squared scattering vector q^2 for selected temperatures. The measured half-widths are not constant but show a strong q^2-dependence especially at higher temperatures. The half-widths do not intercept zero but approach a constant value at $q^2 \to 0$ which results from the effect of confinement on the observed

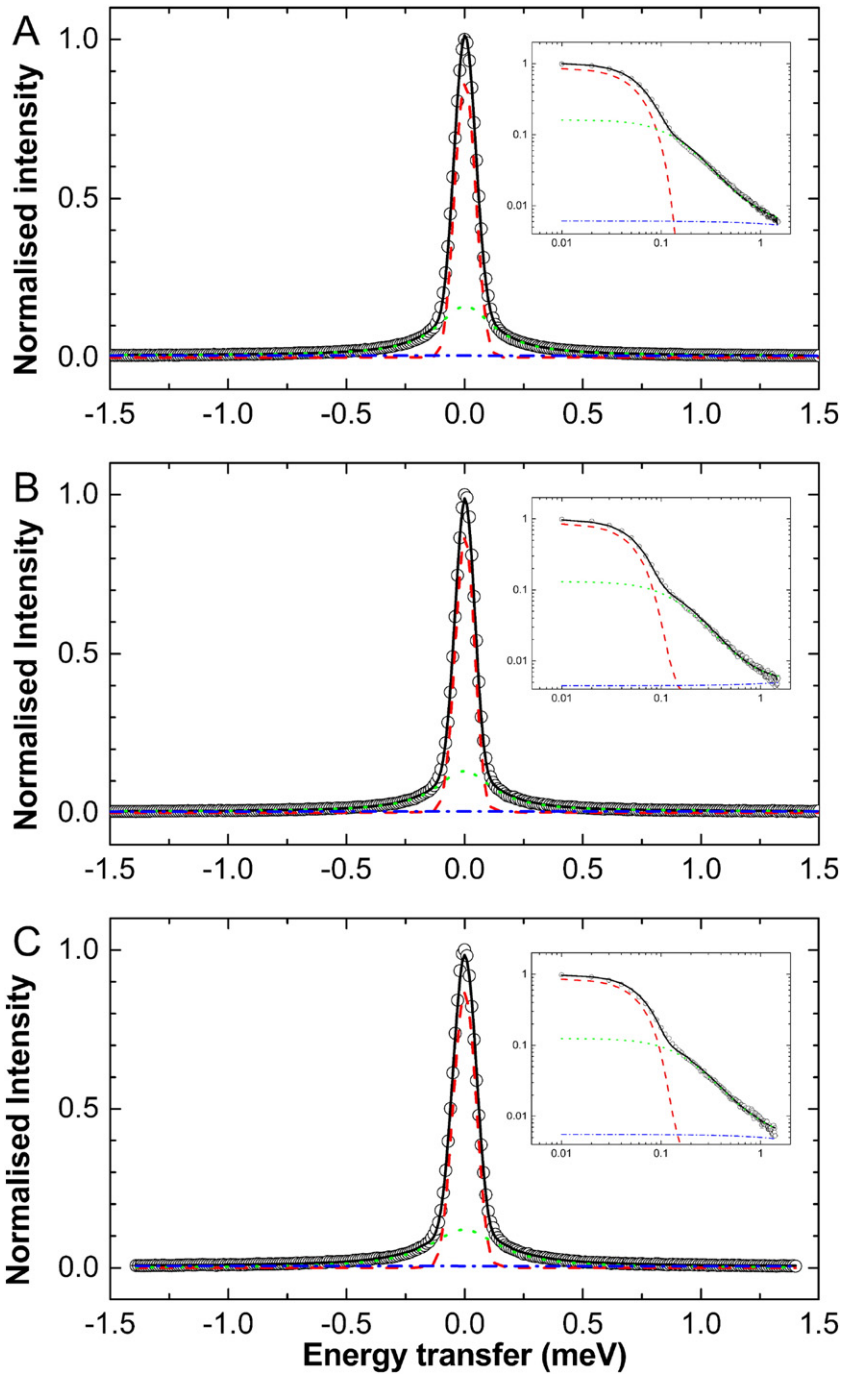

Fig. 1. Quasielastic neutron spectra at the scattering vector $q = 1.8$ Å^{-1}. (A) platypus Hb at 285 K, (B) chicken Hb at 286 K, and (C) crocodile Hb at 285 K. The circles are measured data and the black solid line presents the total fit to the data. The components correspond to the elastic fraction (red dashed line), the Lorentzian (green dotted line) and the linear background (blue dashed-dotted line). The insets in the figures show the data in a log–log plot to illustrate the quality of the fits.

dynamics [19]. The broadening of the half-widths can be described phenomenologically by a simple jump-diffusion model according to

$$\Gamma = \frac{\hbar D q^2}{1 + D q^2 \tau} \tag{11}$$

with the residence time between jumps τ and the jump-diffusion coefficient D [19]. The fits shown in Fig. 5 using that model were performed in the q^2-range between 0.64 and 3.24 Å^{-2}. The diffusion coefficients and residence times of the diffusive internal motions obtained from the HWHM are given as Arrhenius plots in Fig. 8A and C, respectively. Activation energies were extracted from the temperature behaviour of the diffusion coefficients and of the residence times and are given in Table 2. Jump-lengths l were calculated according to

$$l = \sqrt{6D\tau} \tag{12}$$

and are given in Fig. 8E.

In summary, the behaviour of the EISF and of the quasielastic broadening is in agreement with localized diffusive motions within the protein.

As the simple approach following Eq. (2) demonstrated that localized diffusive motions are observed, we tested if the Kneller–Volino model for Brownian dynamics in a quasi-harmonic potential would

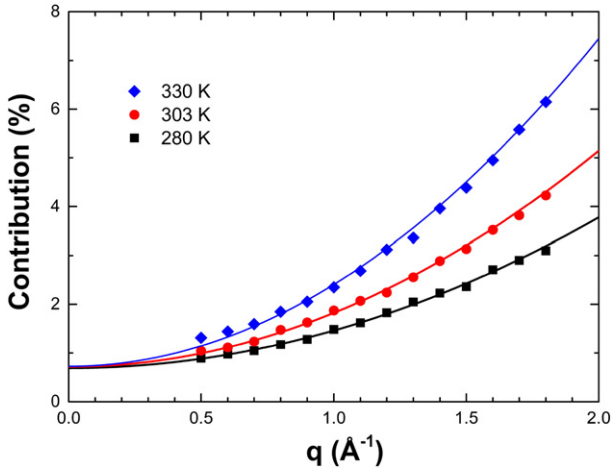

Fig. 2. Contribution of the flat background to the measured spectra. Data shown are from platypus Hb measured on TOFTOF. The solid lines indicate the q^2-dependence.

allow further information to be derived from the quasielastic broadening. The theoretical model function (Eq. (5)) was fitted simultaneously to the whole dataset at each temperature (global fitting procedure). The free parameters for the diffusive motions in confinement were the MSD, the fraction of immobile hydrogens, the diffusion coefficient and the residence time between jumps. In the case that the diffusive motions would be described by a q-independent diffusion coefficient, the fits would have just given a value of $\tau \rightarrow 0$. The theoretical model gave an excellent description of the measured QENS of all investigated samples. As a representative example the fit with the model and the experimental data of platypus Hb at 303 K are shown in Fig. 6. The obtained $<x^2>$ from the samples are given in Fig. 7. In contrast to the simple one Lorentzian analysis described in the previous section the MSD are not only determined from the EISF, but from the full QENS spectra. Effective force constants $<k'>$ were determined from the slope of the $<x^2>$ versus temperature and are compared in Table 1 to the force constants

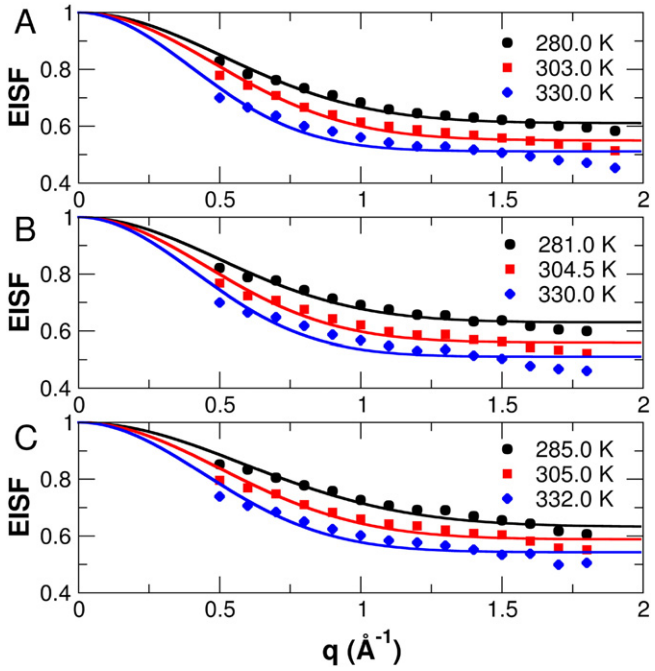

Fig. 3. Elastic incoherent structure factor obtained from the simple one Lorentzian analysis. The solid lines are fits with the Gaussian approximation. (A) Platypus Hb, (B) chicken Hb, (C) crocodile Hb.

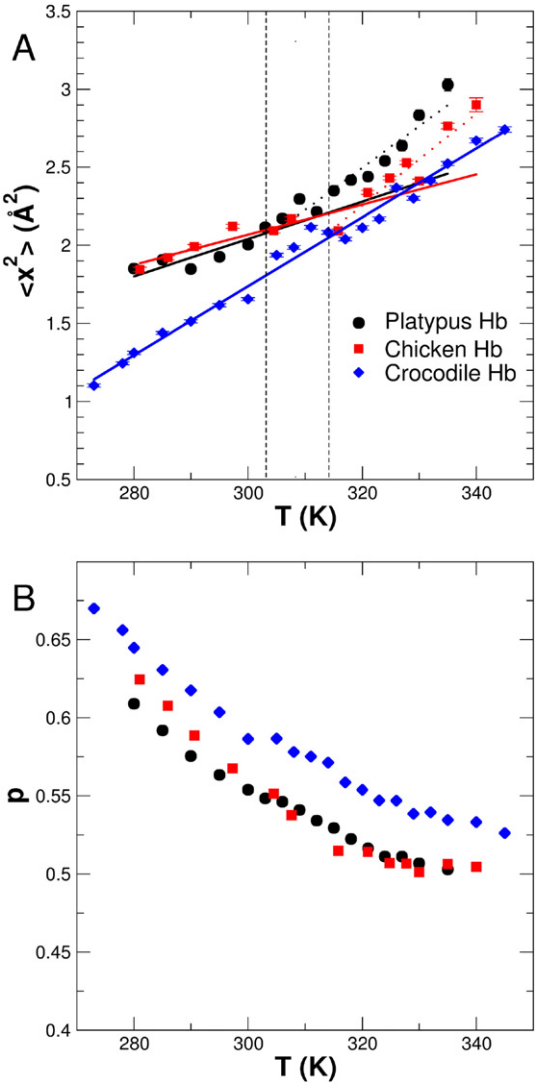

Fig. 4. (A) Mean square displacements and (B) fractions of immobile hydrogens obtained from the simple one Lorentzian analysis. The errors are smaller than the symbols. The vertical dashed lines in (A) indicate the body temperatures from platypus and chicken at 306.2 and 314.2 K (33 and 41 °C), respectively. The solid and dotted lines in (A) are linear fits to the data.

determined from the simple one Lorentzian analysis. The diffusion coefficients, residence times of the diffusive internal motions and jump-lengths obtained with the Brownian model are given in Fig. 8B, D and F, respectively. Activation energies were extracted from the temperature behaviour of the diffusion coefficients and of the residence times and are given in Table 2.

4. Discussion

The structures of human and chicken Hb have been solved by X-ray crystallography showing a high structural similarity of both proteins [34,35]. The crystal structures of salt water crocodile and platypus Hb are not available. The amino acid sequence of salt water crocodile is not published. As a compromise, we used the amino acid sequence of the Nile crocodile, which is a very close relative [36]. Both crocodile proteins are expected to be similar in their sequences and in their secondary structures. The aligned sequences and the predicted α-helical regions of all proteins are shown in Fig. 9. Seven α-helical regions are predicted both for the α- and β-subunits of the proteins. Note that the crystal structures show eight helices. The length and location of the predicted regions are nearly identical for all proteins. The sequence

Table 1
Effective force constants obtained from the measured mean square displacements.

	<k'> (N/m) low temp. range	<k'> (N/m) high temp. range	<k'> (N/m) Brownian oscillator	<k'> (N/m) Brownian oscillator high temp. range
Platypus Hb	0.038 ± 0.004	0.017 ± 0.001	0.0227 ± 0.0003	–
Chicken Hb	0.048 ± 0.002	0.016 ± 0.001	0.039 ± 0.002	0.021 ± 0.002
Crocodile Hb	0.0208 ± 0.0001	–	0.0215 ± 0.0002	–

alignments demonstrate that all proteins share a large amount of similar and identical amino acids. However, there are also a considerable number of non-similar amino acids distributed in the sequences. Regions with a larger number of non-similar amino acids are located before and in the first predicted helix of the α -and β-subunits, in the small loop between the predicted helices F and G of the α-subunit and in the large loop between the predicted helices C and D of the β-subunit.

In previous work we investigated the dynamics of human Hb in red blood cells and as concentrated solution using QENS [10,12]. It could be shown that human Hb undergoes a softening above human body temperature [7], which is visible by a break in the amplitudes of motion close to that temperature. The softening of human Hb is accompanied by a loss of secondary structure, which occurs at body temperature [5,6]. That loss of secondary structure content at body temperature was not found to be limited to human Hb, but also occurs in Hb from a large variety of different species [5,6]. On the picosecond time-scale the structure of human Hb at temperatures above body temperature was found to be less resilient (softer) than the low temperature conformation. Body temperature sensing appears to be imprinted into the physical properties of Hb [7]. Thermal stability, for example, of platypus Hb is significantly reduced compared to chicken and crocodile Hb, which both have similar thermal stability [13]. That behaviour was found to be correlated with weaker forces in platypus Hb as compared to the more thermostable chicken and crocodile Hb on the 0.1 ns time-scale [13].

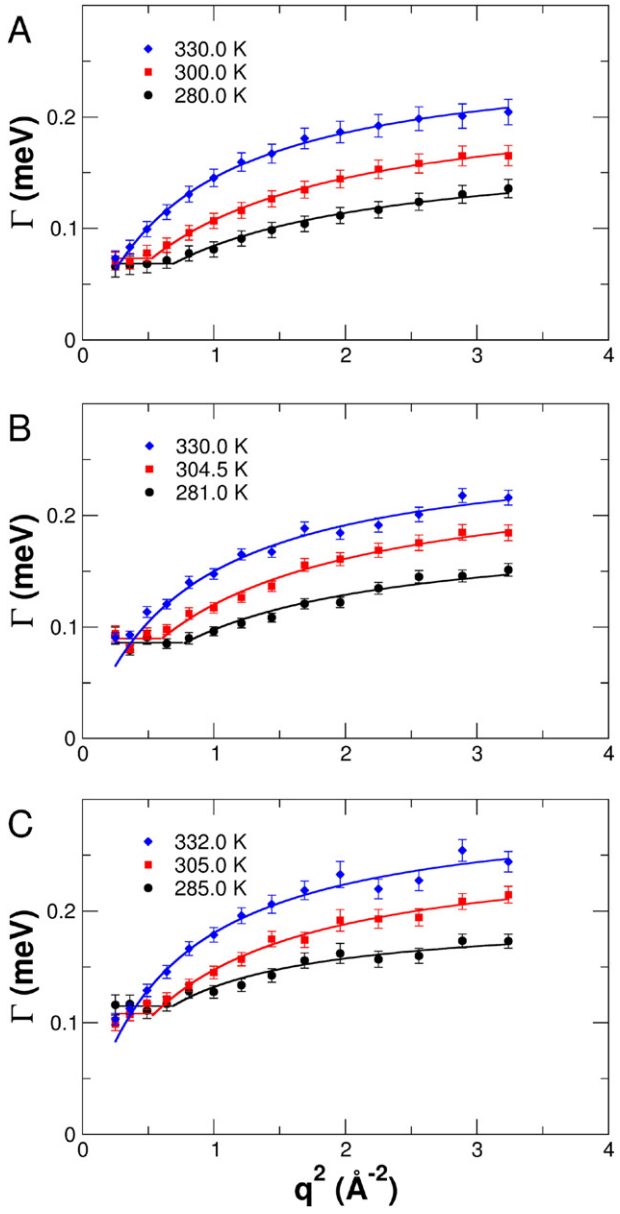

Fig. 5. Half-widths at half-maximum Γ of the Lorentzian as a function of the scattering vector. The solid lines are fits according to a jump-diffusion model in the range of $0.64 \leq q^2 \leq 3.24$ Å^{-2}. The horizontal solid lines indicate the region of constant half-widths.

In this study we investigated, if picosecond dynamics of other members of the Hb family also show characteristic features. Motions of non-exchanged hydrogens are seen by QENS. In the experimentally accessible time window these non-exchanged hydrogens act as reporter atoms for the diffusive motions of amino acid side chains. Side chain motions in proteins contain a strong non-vibrational liquid-like diffusive and confined component. That observation was found by neutron scattering [37] and confirmed later by computer simulations [38,39]. More recently it was also shown by NMR [40]. Pure vibrational motion is contained in our models by a Debye–Waller factor as a prefactor of the equations. Therefore, the reported mean square displacements in our manuscript report on the confined liquid-like diffusive motions. It has been shown in a large number of publications that the quasielastic broadening of proteins measured by neutron time-of-flight spectroscopy can be described effectively by a single Lorentzian [41–49]. The model of a simple single Lorentzian is in that sense useful and justified, as it allows a direct comparison of the different experimental results. In a first approach we interpret the observable motions in terms of a phenomenological average relaxation process, which can be described by a single Lorentzian. Our results should be considered as phenomenological results. It is, however, in general completely unrealistic to assume that all dynamic processes in proteins are characterized only by a single relaxation rate. Mean square displacements, for example, measured by neutron scattering depend very strongly on the instrumental energy resolution [50,51]. The present study concerning fast picosecond dynamics in Hb is a continuation of previous work, where we investigated the dynamics of Hb from different species on the slower 0.1 ns time scale [13].

The <x^2> and the fraction of protons participating in the observed picosecond motions, compare Fig. 4, show clear differences between the investigated samples. Fewer hydrogen atoms participate in the

Table 2
Activation energies from Arrhenius plots of the residence times and diffusion coefficients of fast diffusive motions from the jump-diffusion model and the Brownian oscillator.

	E_a τ (kJ/mol) jump-diff.	E_a D (kJ/mol) jump-diff.	E_a τ (kJ/mol) Brown. osc.	E_a D (kJ/mol) Brown. osc.
Platypus Hb	4.1 ± 0.3	11.5 ± 0.5	5.3 ± 0.4	11.9 ± 0.3
Chicken Hb	4.2 ± 0.2	9.1 ± 0.3	4.7 ± 0.2	9.4 ± 0.1
Crocodile Hb	4.6 ± 0.2	7.9 ± 0.3	6.4 ± 0.1	9.1 ± 0.1

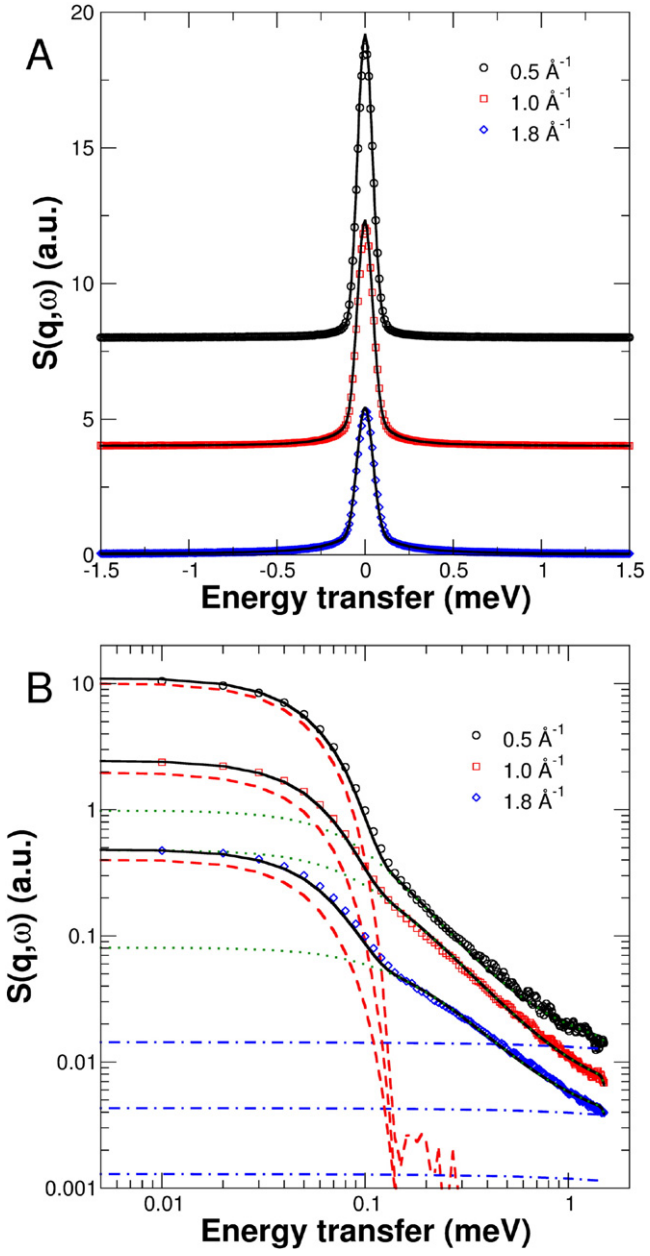

Fig. 6. (A) Measured QENS spectra of platypus Hb at 303 K. Solid black lines are fits with the analytical model for Brownian diffusion in a harmonic potential. (B) Log–log plot of the same data to show the quality of the fits of the quasielastic broadening. The red dashed lines are the elastic and the green dotted lines are the quasielastic components of the fit. The blue dashed-dotted lines are linear background.

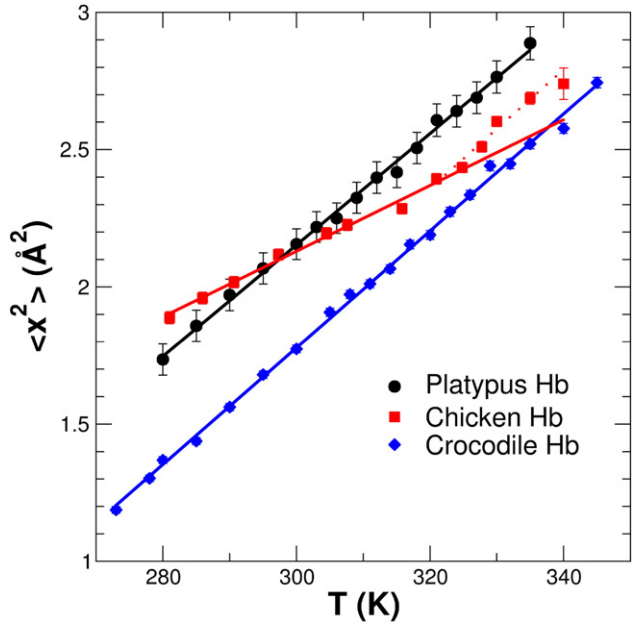

Fig. 7. Mean square displacements of the investigated samples obtained by using the model for Brownian diffusion in a harmonic potential. The lines are linear fits to the $<x^2>$, the dotted line indicates a change in slope of the $<x^2>$ from chicken Hb at high temperatures.

observed motions in crocodile Hb than in platypus and chicken Hb. That observation goes in hand with a lower flexibility of crocodile Hb compared to platypus and chicken Hb over the whole temperature range.

The flexibility of platypus and chicken Hb is nearly identical at temperatures below around 305 K, but differences at higher temperatures emerge, which result in a nearly temperature independent offset of $\Delta<x^2> = 0.23$ Å^2 between both proteins above 315 K. The MSD of both proteins increase linearly up to the body temperatures of the animals. An inflection in the $<x^2>$ is visible, which is shifted by a temperature offset ΔT of approximately 10 °C between platypus and chicken Hb. The inflection is better visible for chicken Hb, but weak and rather smooth for platypus Hb. The locations of the inflection points correlate approximately with the reported average body temperatures of 33 and 41 °C (306.2 and 314.2 K) for platypus and chicken [5], respectively, and the temperature offset ΔT corresponds to the difference between both body temperatures. A similar behaviour was reported for human Hb, although changes in dynamics around body temperature were more pronounced in human Hb [10,12]. As the softening of Hb above body temperature occurs in Hb from very different species, our results support the assumption that the structural softening is a general property of Hb from higher endothermic species. Interestingly, crocodile Hb does not show any inflection point in the $<x^2>$ in the investigated temperature range. The dynamic behaviour of crocodile Hb, therefore, supports the hypothesis that the break in the $<x^2>$ is limited to endotherms but does not exist in exotherms. Molecular forces within the Hb structures were quantified using effective force constants $<k'>$ on the picosecond time-scale. The effective force constants show that the structures of platypus and chicken Hb are rather soft and similar at higher temperatures. In the temperature range below body temperature molecular forces in the structure of platypus Hb are weaker than in chicken Hb. A similar observation was obtained for molecular forces in platypus and chicken Hb on the slower 0.1 ns time-scale [13]. The resilience of crocodile Hb has a value, which is close to that of the soft structures of platypus and chicken Hb at high temperatures. One could speculate that the structural softening is adapted and related to the biological function of the proteins in their physiological environment. Crocodiles live in a broad temperature range, and therefore, it might be necessary for that animal that Hb is kept in the softer conformation over the whole temperature range. Concerning platypus, human and chicken Hb it could be the case that they have been selected by evolution to exist in the softer state only close to their physiological temperatures. These speculations, however, require further strong experimental evidence. Furthermore, our results demonstrate that effective force constants of proteins derived from MSD depend on the time scale under observation. Fast motions of amino acid side chains on the picosecond time scale, studied in this work, are found to be governed by weaker forces than slower motions on the 0.1 ns scale [13].

We now consider the results obtained using the analytic model for Brownian dynamics in a quasi-harmonic potential [25,26]. A similar model was used for the interpretation of diffusive motions of the heme-group in myoglobin measured by Mössbauer spectroscopy [52,53]. Mössbauer spectroscopy is sensitive to very slow diffusive

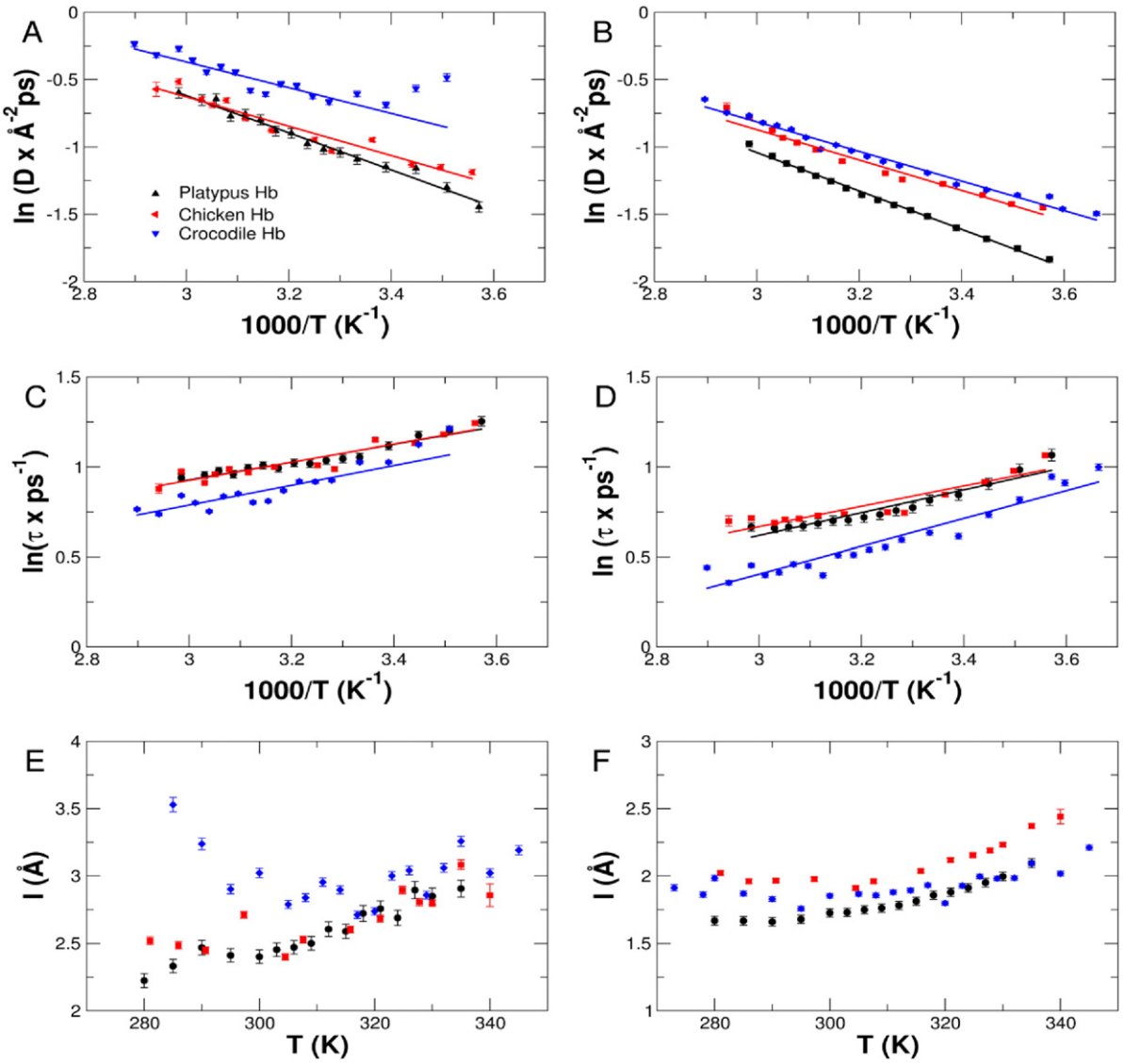

Fig. 8. Arrhenius plots of the diffusion coefficients obtained from (A) the jump-diffusion model and (B) the Brownian oscillator. Arrhenius plots of the residence times determined from (C) the jump-diffusion model and (D) the Brownian oscillator. Jump-lengths from (E) the jump-diffusion model and (F) the Brownian oscillator.

motions faster than 100 ns. Protein dynamics measured by incoherent neutron scattering was interpreted using the viscoelastic Brownian oscillator within the framework of mode coupling theory [37]. The fractional Brownian oscillator was used for the interpretation of picosecond to nanosecond dynamics in proteins measured by neutron scattering [25,54]. In the model for fractional Brownian dynamics a memory function is introduced, which is not the case for the model of Brownian dynamics in a harmonic potential. However, the measured QENS data presented in this work could be described well with the simpler model for Brownian diffusion in a harmonic potential, see Fig. 6. We would like to point out that all samples in this work were measured as highly concentrated protein solutions and not as hydrated protein powders. It could be that picosecond dynamics in proteins deviate from that model at lower hydration levels. Further investigations would be needed to answer that aspect. The shape of the quasielastic scattering is well described by the Brownian oscillator at all measured scattering vectors. Therefore, for simplicity we chose that model for data analysis. The $\langle x^2 \rangle$ obtained from the Brownian oscillator are in good agreement with the $\langle x^2 \rangle$ from the model free analysis. The same strong features in the MSD of the investigated samples are emerging: The flexibility of crocodile Hb is significantly lower compared to both other proteins over the whole temperature range. The $\langle x^2 \rangle$ of platypus and chicken Hb are similar in magnitude at low temperatures below approximately 305 K, but diverge at higher temperatures with a nearly constant offset in the MSDs of $\Delta\langle x^2 \rangle = 0.18$ Å^2 above 315 K. What is not reproduced from the Brownian oscillator is the subtle inflection point in the $\langle x^2 \rangle$ of platypus Hb, whereas it is visible for chicken Hb. Within the Brownian diffusion model the effective force constants of the platypus and crocodile Hb structures are similar, whereas forces in chicken Hb are around 1.7 to 1.8 times larger. At high temperatures the soft structure of chicken Hb has similar resilience as the soft structures of platypus and crocodile Hb. The values of the immobile fraction obtained within the Brownian diffusion model are essentially identical to those from the simple-model analysis described above.

Diffusion coefficients and residence times between molecular jumps were determined from the HWHM using the jump-diffusion model and from the full QENS spectra using the Brownian oscillator. Activation energies were extracted from the temperature dependence. Differences in the diffusivities and residence times are visible for the different samples depending also on the theoretical model used. The diffusion coefficients obtained from the HWHM using the jump-diffusion model are in average around 50% larger than those from the Brownian oscillator. The residence times obtained from the HWHM are in average 35% larger than those from the Brownian oscillator. Diffusion coefficients

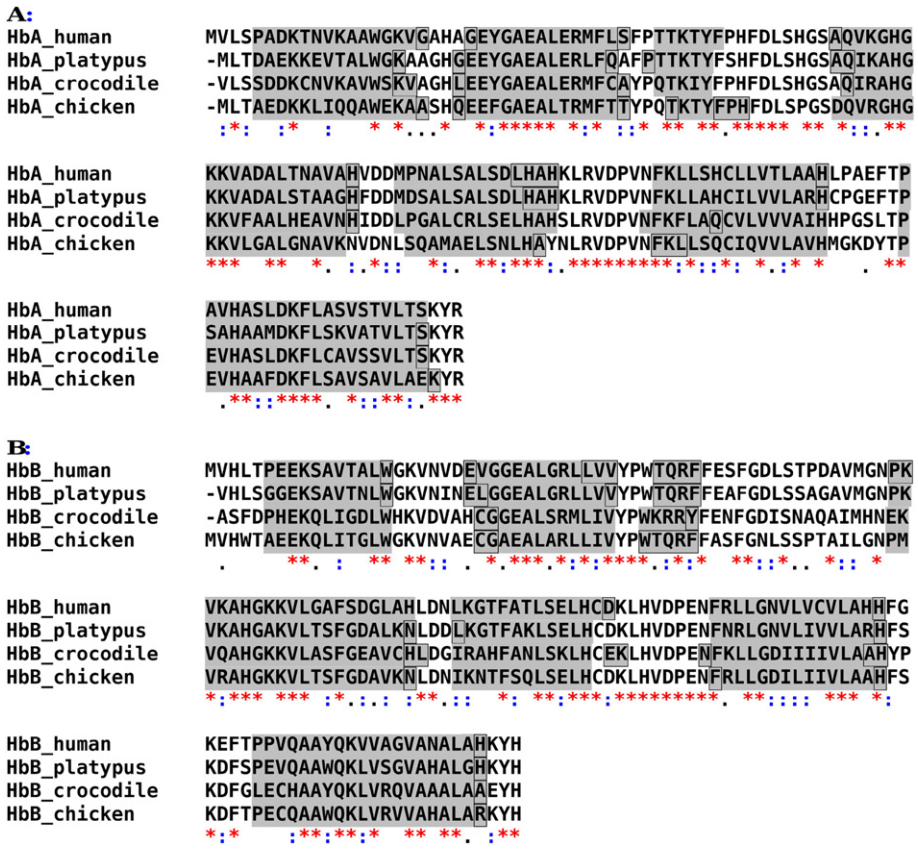

Fig. 9. Sequence alignments of Hb from the different species. The (A) α-subunits and (B) β-subunits. The amino acid similarity between all proteins is given as follows: asterisks indicate identical amino acids, colons indicate similar amino acids and empty space represents absence or low degree of similarity. The grey background indicates predicted α-helical contents of the subunits. Black frames label the parts of predicted helices where the prediction confidence was less than 50%. The figure was also shown in [13].

calculated from the HWHM and from the Brownian oscillator are lower for platypus Hb than for crocodile Hb. The diffusivity of chicken Hb is found between the other proteins depending on the model used. Residence times between jumps determined from both the HWHM and from the Brownian oscillator are shorter in crocodile Hb than in platypus and chicken Hb, which show similar behaviour. The jump-lengths inform about the lengths of the atomistic jumps of the side chains. They increase slightly with temperature and are in a similar range for the different proteins. The parameters of crocodile Hb obtained from the HWHM using the jump-diffusion model show unphysical deviations at the lowest temperatures, whereas the Brownian oscillator yields a coherent picture of all samples at all temperatures. The values of the activation energies from the diffusion coefficients are in reasonable agreement independent of the theoretical model used. The activation energies from the residence times of the jump-diffusion model are slightly underestimated as compared to those from the Brownian oscillator. For crocodile Hb the activation energies of the jump-diffusion model are in general a bit underestimated, which is related to the deviations at lowest temperatures.

We now turn our attention to the interpretation and the origin of the measured dynamics. Picosecond dynamics of hydrated proteins were interpreted to arise from fast rotational and librational motions of amino acid side chains along the consecutive C – C bonds [55,56]. The fraction of mobile hydrogen atoms was attributed to side chains of amino acids located on the surface of the protein, while the fraction of immobile hydrogen atoms would correspond to buried residues [55,56]. Therefore, the amino acids of the measured fraction of mobile hydrogen atoms consist mostly of polar and charged amino acids, as these are the predominating component of surface residues. Correlation times of rotamer transitions of side chains were investigated using molecular dynamics simulations [57]. The rotamer correlation times showed a strong decrease on the surface of the protein and a weaker decrease for dihedral angles located away from the main chain in support of the view given by Zanotti and coworkers [55,56]. Therefore, our interpretation is that the picosecond motions observed in this work correspond to fast torsional jumps between different rotamer orientations of the amino acid side chains. The observed mobile side chains are mostly those located on the surface of the protein. The measured fractions of mobile hydrogen atoms can be used to visualize the amino acids belonging to the mobile surface layer. The solvent accessible surface area of the amino acids of the chicken Hb structure (PDB code 1HBR) was calculated using the MMTK toolkit [58]. The fraction of mobile hydrogens was then calculated as the number of hydrogens in residues having a solvent accessible surface area larger than a certain cut-off value divided by the total number of hydrogens in the protein. The cut-off values were 0.138 nm^2/atom and 0.190 nm^2/atom yielding the measured fractions of mobile hydrogens of 0.37 at 281 K and of 0.5 at 340 K, respectively. The amino acids of chicken Hb possibly accounting for the measured fraction of mobile hydrogens at 281 and 340 K are shown in Fig. 10. They appear to form a clustered network on the surface of the protein. With increasing temperature deeper buried amino acids contribute to mobile surface layer.

Interactions between side chains are governed by van der Waals, hydrogen bonding and by screened electrostatic interactions. Hydrophobic side chains in the protein interior interact with each other via weak van der Waals interactions. Charged residues can interact via ionic bonds and polar residues can form hydrogen bonds with each other and with the solvent. As discussed before charged and polar groups are predominantly located on the protein surface and are assumed to contribute to the measured fraction of mobile hydrogens. The temperature dependence of the residence times and of the diffusion coefficients can be used to quantify the interactions of side chains of the

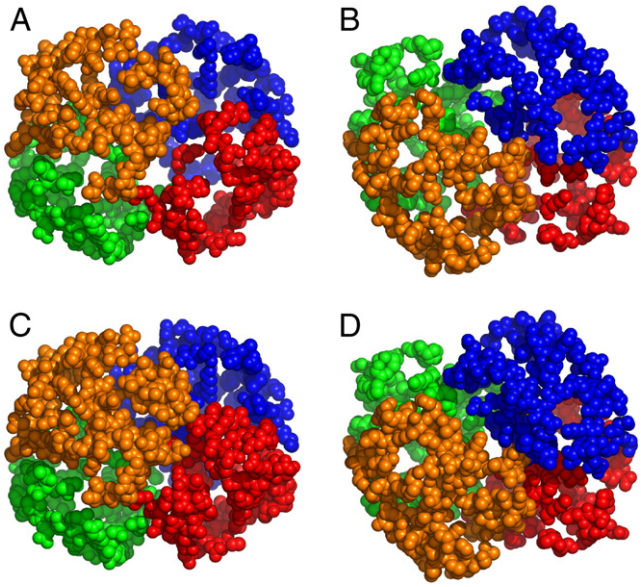

Fig. 10. Surface residues of chicken Hb possibly contributing to the measured fractions of mobile hydrogens. (A) and (B) Surface residues at 281 K. (C) and (D) Surface residues at 340 K. The images on the right side of the figure are rotated horizontally by 90°. Residues belonging to separate chains are marked by different colours.

mobile surface residues. The activation energy of the residence times is a measure of the average energy, which is needed for an individual side chain to break free out of its bonded configuration, while the activation energy of the diffusion coefficient is a measure of the energy, which is needed to displace other groups and to free sufficient space for the displacement of the individual side chain. Both processes do not necessarily have the same energetics. Within the errors the activation energies of the residence times and of the diffusion coefficients are similar between the different samples and have the average values of 5.5 kJ/mol for the residence times of the Brownian oscillator (4.3 kJ/mol for the residence times of the jump-diffusion model), and 10.1 kJ/mol for the diffusion coefficient of the Brownian oscillator (9.5 kJ/mol for the diffusion coefficients of the jump-diffusion model). The results show that the energy, which is required to displace other side chains, is nearly twice than that, which is needed for an individual side chain to break free. Peters et al. [59] determined activation energies of native and inhibited human acetylcholinesterase of 12.25 and 12.62 kJ/mol, respectively, from measured MSD on the same time-scale as in this study. The activation energy obtained from the diffusion coefficients is in agreement with these results. The explanation is that both measurements inform about the displacements of the side chains. Activation energies for the rupture of a hydrogen bond in a β-sheet and in an α-helix in hydrated environment were calculated to be 6.61 and 8.08 kJ/mol, respectively [60]. Our results show that attractive and repulsive forces between side chains on the picosecond time scale are very effectively counterbalanced. The determined activation energies are close to the energy, which is required for the rupture of a single hydrogen bond in a protein.

5. Conclusion

In this study we investigated internal dynamics of Hb from different species on the picosecond time-scale using incoherent neutron scattering. The measured QENS data were interpreted within a simple one Lorentzian fit approach and with the Kneller–Volino model of Brownian diffusion in a quasi-harmonic potential. Variations in the amino acid sequence of the proteins were found to modify the MSD, diffusion coefficients and residence times. Our results demonstrate that picosecond dynamics in proteins are not only controlled by strong external parameters such as the viscosity of the solvent [61,62] or the hydration level [49,63–66], but also depend on specific physicochemical properties and interactions of amino acids, even when the proteins are structurally very similar. The results from the simple one Lorentzian analysis support the hypothesis that Hb shows a structural softening close to body temperature of endotherms, which does not occur in exotherms. Activation energies of local side chain dynamics were found to be similar between the different proteins.

Acknowledgements

A.M.S. thanks Prof. Dieter Richter for continuous support. Platypus RBC was provided by Nick Gust (Department of Primary Industries Tasmania, Australia) and Dominic Geraghty (University of Tasmania, Australia). Crocodile blood was provided by Crocodylus Park (Darwin, Australia). We thank Prof. Philip Kuchel (University of Sydney, Australia) for the use of his laboratory to purify crocodile and platypus Hb. Chicken blood was provided by Mario Suárez Avello and Josefa García Álvarez. This work is based on experiments performed at the Institute Laue-Langevin (ILL), Grenoble, France, at the Forschungs-Neutronenquelle Heinz Maier-Leibnitz (MLZ), Garching, Germany, and at the Paul Scherrer Institute (PSI), Villigen, Switzerland.

References

[1] W.A. Eaton, E.R. Henry, J. Hofrichter, A. Mozzarelli, Is cooperative oxygen binding by hemoglobin really understood? Nat. Struct. Biol. 6 (1999) 351–358.
[2] J. Monod, J. Wyman, J.-P. Changeux, On the nature of allosteric transitions: a plausible model, J. Mol. Biol. 12 (1965) 88–118.
[3] D.E. Koshland, G. Némethy, D. Filmer, Comparison of experimental binding data and theoretical models in proteins containing subunits, Biochemistry 5 (1966) 365–385.
[4] M.F. Perutz (Ed.), Science is Not a Quiet Life: Unravelling the Atomic Mechanism of Haemoglobin, World Scientific Publishing, Singapore, 1998.
[5] K.F.T. Zerlin, N. Kasischke, I. Digel, C. Maggakis-Kelemen, A. Temiz Artmann, D. Porst, et al., Structural transition temperature of hemoglobins correlates with species' body temperature, Eur. Biophys. J. 37 (2007) 1–10.
[6] I. Digel, C. Maggakis-Kelemen, K.F. Zerlin, P. Linder, N. Kasischke, P. Kayser, et al., Body temperature-related structural transitions of monotremal and human hemoglobin, Biophys. J. 91 (2006) 3014–3021.
[7] G.M. Artmann, I. Digel, K.F. Zerlin, C. Maggakis-Kelemen, P. Linder, D. Porst, et al., Hemoglobin senses body temperature, Eur. Biophys. J. 38 (2009) 589–600.
[8] G.M. Artmann, C. Kelemen, D. Porst, G. Büldt, S. Chien, Temperature transitions of protein properties in human red blood cells, Biophys. J. 75 (1998) 3179–3183.
[9] A.M. Stadler, R. Schweins, G. Zaccai, P. Lindner, Observation of a large-scale superstructure in concentrated hemoglobin solutions by using small angle neutron scattering, J. Phys. Chem. Lett. 1 (2010) 1805–1808.
[10] A.M. Stadler, I. Digel, G.M. Artmann, J.P. Embs, G. Zaccai, G. Büldt, Hemoglobin dynamics in red blood cells: correlation to body temperature, Biophys. J. 95 (2008) 5449–5461.
[11] A.M. Stadler, L. van Eijck, F. Demmel, G. Artmann, Macromolecular dynamics in red blood cells investigated using neutron spectroscopy, J. R. Soc. Interface 8 (2011) 590–600.
[12] A.M. Stadler, I. Digel, J.P. Embs, T. Unruh, M. Tehei, G. Zaccai, et al., From powder to solution: hydration dependence of human hemoglobin dynamics correlated to body temperature, Biophys. J. 96 (2009) 5073–5081.
[13] A.M. Stadler, C.J. Garvey, A. Bocahut, S. Sacquin-Mora, I. Digel, G.J. Schneider, et al., Thermal fluctuations of haemoglobin from different species: adaptation to temperature via conformational dynamics, J. R. Soc. Interface 9 (2012) 2845–2855.
[14] G. Zaccai, How soft is a protein? A protein dynamics force constant measured by neutron scattering, Science 288 (2000) 1604–1607 (80-.).
[15] A. Ostermann, R. Waschipky, F.G. Parak, G.U. Nienhaus, Ligand binding and conformational motions in myoglobin, Nature 404 (2000) 205–208.
[16] J.A. McCammon, S.C. Harvey, Dynamics of Proteins and Nucleic Acids, Cambridge University Press, Cambridge New York Melbourne, 1987.
[17] J. Fitter, T. Gutberlet, J. Katsaras (Eds.), Neutron Scattering in Biology — Techniques and Applications, Springer Berlin Heidelberg New York, Berlin Heidelberg, 2006.
[18] V. Garcia-Sakai, C. Alba-Simionesco, S.H. Chen (Eds.), Dynamics of Soft Matter — Neutron Applications, Springer New York Dordrecht Heidelberg London, New York Dordrecht Heidelberg London, 2012.
[19] M. Bée, Quasielastic Neutron Scattering: Principles and Applications in Solid State Chemistry, Biology, and Materials Science, Adam Hilger, Bristol and Philadelphia, 1988.
[20] V.F. Sears, Neutron scattering lengths and cross sections, Neutron News 3 (1992) 26–37.
[21] E. DeMoll, D.J. Cox, E. Daniel, A.F. Riggs, Apparent specific volume of human hemoglobin: effect of ligand state and contribution of heme, Anal. Biochem. 363 (2007) 196–203.
[22] The ILL Yellow Book, http://www.ill.eu/instruments-Support/instruments-Groups/yellowbook/.

[23] W. Häußler, O. Holderer, T. Unruh, J. Wuttke, High-resolution neutron spectroscopy at the FRM II, Neutron News 22 (2011) 24–30.
[24] J. Mesot, S. Janssen, L. Holitzner, R. Hempelmann, Focus: project of a space and time focussing time-of-flight spectrometer for cold neutrons at the spallation source SINQ of the Paul Scherrer Institute, J. Neutron Res. 3 (1996) 293–310.
[25] G.R. Kneller, Quasielastic neutron scattering and relaxation processes in proteins: analytical and simulation-based models, Phys. Chem. Chem. Phys. 7 (2005) 2641–2655.
[26] F. Volino, J.-C. Perrin, S. Lyonnard, Gaussian model for localized translational motion: application to incoherent neutron scattering, J. Phys. Chem. B 110 (2006) 11217–11223.
[27] D.J. Bicout, G. Zaccai, Protein flexibility from the dynamical transition: a force constant analysis, Biophys. J. 80 (2001) 1115–1123.
[28] J.D. Thompson, D.G. Higgins, T.J. Gibson, CLUSTAL W: improving the sensitivity of progressive multiple sequence alignment through sequence weighting, position-specific gap penalties and weight matrix choice, Nucleic Acids Res. 22 (1994) 4673–4680.
[29] C. Cole, J.D. Barber, G.J. Barton, The Jpred 3 secondary structure prediction server, Nucleic Acids Res. 36 (2008) W197–W201.
[30] G. Gibrat, F.L. Assairi, Y. Blouquit, C.T. Craescu, M.-C. Bellissent-Funel, Biophysical study of thermal denaturation of apo-calmodulin: dynamics of native and unfolded states, Biophys. J. 95 (2008) 5247–5256.
[31] D. Russo, J. Pérez, J.-M. Zanotti, M. Desmadril, D. Durand, Dynamic transition associated with the thermal denaturation of a small beta protein, Biophys. J. 83 (2002) 2792–2800.
[32] J. Peters, G.R. Kneller, Motional heterogeneity in human acetylcholinesterase revealed by a non-Gaussian model for elastic incoherent neutron scattering, J. Chem. Phys. 139 (2013) 165102.
[33] A.M. Stadler, T. Unruh, K. Namba, F. Samatey, G. Zaccai, Correlation between supercoiling and conformational motions of the bacterial flagellar filament, Biophys. J. 105 (2013) 2157–2165.
[34] J.E. Knapp, M.A. Oliveira, Q. Xie, S.R. Ernst, A.F. Riggs, M.L. Hackert, The structural and functional analysis of the hemoglobin D component from chicken, J. Biol. Chem. 274 (1999) 6411–6420.
[35] B. Shaanan, Structure of human oxyhaemoglobin at 2.1 Å resolution, J. Mol. Biol. 171 (1983) 31–59.
[36] R.W. Meredith, E.R. Hekkala, G. Amato, J. Gatesy, A phylogenetic hypothesis for *Crocodylus* (Crocodylia) based on mitochondrial DNA: evidence for a trans-Atlantic voyage from Africa to the New World, Mol. Phylogenet. Evol. 60 (2011) 183–191.
[37] W. Doster, S. Cusack, W. Petry, Dynamic instability of liquidlike motions in a globular protein observed by inelastic neutron scattering, Phys. Rev. Lett. 65 (1990) 1080–1083.
[38] G.R. Kneller, J.C. Smith, Liquid-like side-chain dynamics in myoglobin, J. Mol. Biol. 242 (1994) 181–185.
[39] S. Dellerue, A.J. Petrescu, J.C. Smith, M.C. Bellissent-Funel, Radially softening diffusive motions in a globular protein, Biophys. J. 81 (2001) 1666–1676.
[40] K. Lindorff-Larsen, R.B. Best, M.A. Depristo, C.M. Dobson, M. Vendruscolo, Simultaneous determination of protein structure and dynamics, Nature 433 (2005) 128–132.
[41] K. Yoshida, K. Vogtt, Z. Izaola, M. Russina, T. Yamaguchi, M.-C. Bellissent-Funel, Alcohol induced structural and dynamic changes in β-lactoglobulin in aqueous solution: a neutron scattering study, Biochim. Biophys. Acta 1824 (2012) 502–510.
[42] M.-S. Appavou, G. Gibrat, M.-C. Bellissent-Funel, Temperature dependence on structure and dynamics of Bovine Pancreatic Trypsin Inhibitor (BPTI): a neutron scattering study, Biochim. Biophys. Acta 1794 (2009) 1398–1406.
[43] A.M. Gaspar, M.-S. Appavou, S. Busch, T. Unruh, W. Doster, Dynamics of well-folded and natively disordered proteins in solution: a time-of-flight neutron scattering study, Eur. Biophys. J. 37 (2008) 573–582.
[44] J. Fitter, J. Heberle, Structural equilibrium fluctuations in mesophilic and thermophilic alpha-amylase, Biophys. J. 79 (2000) 1629–1636.
[45] Z. Bu, D.A. Neumann, S.H. Lee, C.M. Brown, D.M. Engelman, C.C. Han, A view of dynamics changes in the molten globule-native folding step by quasielastic neutron scattering, J. Mol. Biol. 301 (2000) 525–536.
[46] G. Schirò, M. Sclafani, C. Caronna, F. Natali, M. Plazanet, A. Cupane, Dynamics of myoglobin in confinement: an elastic and quasi-elastic neutron scattering study, Chem. Phys. 345 (2008) 259–266.
[47] M. Jasnin, M. Moulin, M. Haertlein, G. Zaccai, M. Tehei, In vivo measurement of internal and global macromolecular motions in *Escherichia coli*, Biophys. J. 95 (2008) 857–864.
[48] M. Tehei, J.C. Smith, C. Monk, J. Ollivier, M. Oettl, V. Kurkal, et al., Dynamics of immobilized and native *Escherichia coli* dihydrofolate reductase by quasielastic neutron scattering, Biophys. J. 90 (2006) 1090–1097.
[49] J. Pieper, T. Hauss, A. Buchsteiner, K. Baczyński, K. Adamiak, R.E. Lechner, et al., Temperature- and hydration-dependent protein dynamics in photosystem II of green plants studied by quasielastic neutron scattering, Biochemistry 46 (2007) 11398–11409.
[50] K. Wood, C. Caronna, P. Fouquet, W. Haussler, F. Natali, J. Ollivier, et al., A benchmark for protein dynamics: ribonuclease A measured by neutron scattering in a large wavevector-energy transfer range, Chem. Phys. 345 (2008) 305–314.
[51] H. Nakagawa, H. Kamikubo, M. Kataoka, Effect of conformational states on protein dynamical transition, Biochim. Biophys. Acta 1804 (2010) 27–33.
[52] F. Parak, E.W. Knapp, D. Kucheida, Protein dynamics: Mössbauer spectroscopy on deoxymyoglobin crystals, J. Mol. Biol. 161 (1982) 177–194.
[53] F.G. Parak, Physical aspects of protein dynamics, Rep. Prog. Phys. 66 (2003) 103–129.
[54] V. Calandrini, V. Hamon, K. Hinsen, P. Calligari, M.-C. Bellissent-Funel, G.R. Kneller, Relaxation dynamics of lysozyme in solution under pressure: combining molecular dynamics simulations and quasielastic neutron scattering, Chem. Phys. 345 (2008) 289–297.
[55] J.M. Zanotti, M.C. Bellissent-Funel, J. Parello, Hydration-coupled dynamics in proteins studied by neutron scattering and NMR: the case of the typical EF-hand calcium-binding parvalbumin, Biophys. J. 76 (1999) 2390–2411.
[56] J.-M. Zanotti, G. Hervé, M.-C. Bellissent-Funel, Picosecond dynamics of T and R forms of aspartate transcarbamylase: a neutron scattering study, Biochim. Biophys. Acta 1764 (2006) 1527–1535.
[57] A.D. Scouras, V. Daggett, The dynameomics rotamer library: amino acid side chain conformations and dynamics from comprehensive molecular dynamics simulations in water, Protein Sci. 20 (2011) 341–352.
[58] K. Hinsen, The molecular modeling toolkit: a new approach to molecular simulations, J. Comput. Chem. 21 (2000) 79–85.
[59] M. Trapp, M. Trovaslet, F. Nachon, M.M. Koza, L. van Eijck, F. Hill, et al., Energy landscapes of human acetylcholinesterase and its huperzine A-inhibited counterpart, J. Phys. Chem. B 116 (2012) 14744–14753.
[60] S.-Y. Sheu, D.-Y. Yang, H.L. Selzle, E.W. Schlag, Energetics of hydrogen bonds in peptides, Proc. Natl. Acad. Sci. U. S. A. 100 (2003) 12683–12687.
[61] E. Cornicchi, G. Onori, A. Paciaroni, Picosecond-time-scale fluctuations of proteins in glassy matrices: the role of viscosity, Phys. Rev. Lett. 95 (2005) 158104.
[62] E. Cornicchi, M. Marconi, G. Onori, A. Paciaroni, Controlling the protein dynamical transition with sugar-based bioprotectant matrices: a neutron scattering study, Biophys. J. 91 (2006) 289–297.
[63] A. Paciaroni, A. Orecchini, S. Cinelli, G. Onori, R.E. Lechner, J. Pieper, Protein dynamics on the picosecond timescale as affected by the environment: a quasielastic neutron scattering study, Chem. Phys. 292 (2003) 397–404.
[64] U. Lehnert, V. Réat, M. Weik, G. Zaccaï, C. Pfister, Thermal motions in bacteriorhodopsin at different hydration levels studied by neutron scattering: correlation with kinetics and light-induced conformational changes, Biophys. J. 75 (1998) 1945–1952.
[65] K. Wood, U. Lehnert, B. Kessler, G. Zaccai, D. Oesterhelt, Hydration dependence of active core fluctuations in bacteriorhodopsin, Biophys. J. 95 (2008) 194–202.
[66] J. Fitter, The temperature dependence of internal molecular motions in hydrated and dry alpha-amylase: the role of hydration water in the dynamical transition of proteins, Biophys. J. 76 (1999) 1034–1042.